

DDS3D: Dense Pseudo-Labels with Dynamic Threshold for Semi-Supervised 3D Object Detection

Jingyu Li^{1*}, Zhe Liu^{1*}, Jinghua Hou¹, Ding kang Liang^{2†}

Abstract—In this paper, we present a simple yet effective semi-supervised 3D object detector named DDS3D. Our main contributions have two-fold. On the one hand, different from previous works using Non-Maximal Suppression (NMS) or its variants for obtaining the sparse pseudo labels, we propose a dense pseudo-label generation strategy to get dense pseudo-labels, which can retain more potential supervision information for the student network. On the other hand, instead of traditional fixed thresholds, we propose a dynamic threshold manner to generate pseudo-labels, which can guarantee the quality and quantity of pseudo-labels during the whole training process. Benefiting from these two components, our DDS3D outperforms the state-of-the-art semi-supervised 3d object detection with mAP of 3.1% on the pedestrian and 2.1% on the cyclist under the same configuration of 1% samples. Extensive ablation studies on the KITTI dataset demonstrate the effectiveness of our DDS3D. The code and models will be made publicly available at <https://github.com/hust-jy/DDS3D>

I. INTRODUCTION

Recently, LiDAR-based 3D Object Detection has received increasing attention in autonomous driving since it can help the car better understand the environment. To achieve satisfactory performance, most existing methods [41], [18], [31] need massive labeled images for training. However, annotating 3D bounding boxes for each object is expensive and laborious. A compromise solution is the Semi-Supervised 3D object Detection (SS3D) paradigm, i.e., using a large number of unlabeled data to boost the performance of a detector trained by a small amount of labeled data.

A pioneer for SS3D is 3DIoUMatch [38], which addresses this task by a teacher-student paradigm, i.e., the student conduct detection training, and the teacher is in charge of annotating pseudo-labels for unlabeled images. 3DIoUMatch proposes a confidence-based label filtering strategy, while the confidence includes IoU estimation and classification score. Additionally, NMS-like post-processing is introduced to balance the quality and quantity of pseudo-labels. Although 3DIoUMatch achieves considerable performance, it needs to take tremendous effort to balance the effect of each component. Such a complex method gives rise to a question: *Can SS3D be solved with a simple pipeline?*

To answer this question, we revisit the existing label filtering strategy and empirically find two interesting phe-

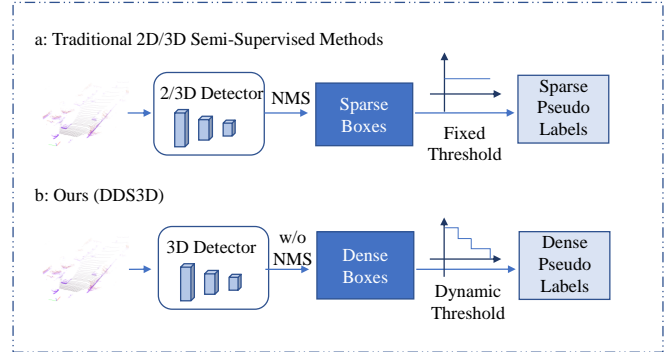


Fig. 1. The comparison of our method and previous methods in terms of pseudo-label generation strategy. (a) Previous methods adopt NMS to generate sparse predictions, and a fixed threshold is used to choose high-quality candidates. (b) The proposed method generates dense predictions and uses a dynamic threshold to make the model better adapted to the quality of the pseudo label.

nomena: 1) NMS is commonly used to filter out duplicate low-scoring predictions, but sparse pseudo-labels are unwise in the semi-supervised objection detection, e.g., NMS easily removes correct supervisory information; 2) Using a fixed threshold (e.g., class or IoU scores) to filter the labels is sub-optimal. Specifically, if the threshold is set to high, the massive pseudo-labels will be regarded as false negatives. Accordingly, by adopting a low fixed threshold, the model will generate massive low-quality pseudo-labels.

In this paper, we dedicate to designing a simple yet effective semi-supervised method to circumvent the above phenomena. Specifically, we first remove the NMS for the teacher’s predictions, which helps to generate dense pseudo-labels. As a result, the model can obtain more supervisory information. Furthermore, we propose a dynamic threshold strategy, i.e., the threshold decreases as the iteration increases. Our intuition is that in the early stage of training, the quality of predicted results from the teacher is unstable, so using a high threshold to slowly improve the precision rate is reasonable. But in the later stages of training, the predicted results from the teacher are reliable, and using a low threshold is beneficial to boost the recall rate. We call such method Dense Pseudo-Labels with Dynamic Threshold for Semi-supervised 3D object detection (DDS3D), and Fig. 1 illustrates the difference between the proposed method and previous works in terms of generating pseudo-labels.

In summary, the main contributions of this paper are two-fold: 1) We deeply analyze the limitations of the current pseudo-label generation strategy for semi-supervised 3D

This work was supported by the Young Scientists Fund of the National Natural Science Foundation of China under Grant 62206103

* Equal contribution

†Corresponding author (dkliang@hust.edu.cn)

¹School of Electronic Information and Communication, Huazhong University of Science and Technology

²School of Artificial Intelligence and Automation, Huazhong University of Science and Technology

object detection. Beside, we point out that the multiple components from the previous filtering label strategy are not essential; 2) We propose a simple yet effective method named DDS3D that uses dense pseudo-labels and a dynamic threshold strategy, which can well guarantee the quality and quantity of pseudo-labels during training.

Extensive experiments are conducted on the KITTI [5] dataset, and significant improvements from the dynamic threshold strategy indicate its effectiveness. In particular, compared with state-of-the-art, when using only 1% of labeled data, our method outperforms 3.1 absolute improvements on the pedestrian and 2.1 absolute improvements on the cyclist.

II. RELATED WORK

3D Object Detection In the past few years, there have been numerous detection methods to deal with 3D object detection [4], [24], [7], [16], [17]. In terms of point cloud representations: point-based [31], [42], [46], [49], [13] and voxel-based [52], [3], [41]. Point-based methods directly consume irregular point clouds to extract features. PointRCNN [31] adopts PointNet++ [23] as the backbone to process point clouds, binary classification to obtain foreground points and regression to generate proposals on obtained foreground points, then the proposals are refined in the second stage with the semantic and spatial information. Voxel-based methods adopt voxelization to make point clouds regular, making it possible to extract features using asymmetric functions, e.g., convolution. VoxelNet [52] adopts 3D convolution to extract features from regular voxels. SECOND [41] replaces the conventional 3D convolution with a 3D submanifold sparse convolution to speed up. TANNet [18] adopts a triplet attention module to make the detection model more robust by considering the feature-wise relationship. CenterPoint [44] implements the center-based method on 3D Object Detection, which considers objects as key points at the heatmap derived from the bird’s-eye-view (BEV) feature. Although the Voxel-based methods are more computationally efficient, the inevitable information loss degrades the fine-grained localization accuracy. Therefore, some methods consider how to combine point clouds and voxels. PV-RCNN [30] proposes the Voxel Set Abstraction (VSA) that integrates multi-scale voxel features into key points, and then the keypoint features are aggregated to the RoI-grid points to learn proposal-specific features for fine-grained proposal refinement and confidence prediction.

Semi-Supervised Learning (SSL) Compared to supervised learning, SSL method can only use a small amount of data, which increases the difficulty of the task. Previous works are mainly divided into two categories of methods, consistency regularization [29], [28], [36], [25], [35] and pseudo-labeling [9], [2], [32]. Temporal Ensembling [29] first proposes consistency regularization and many SSL methods [2], [1] leverage consistency regularization. Mean Teacher [35] takes the teacher model as the exponential moving average (EMA) of the student model and then adopts the consistent regularization to enforce the predictions

on unlabeled data to be consistent under different data augmentations. Others adopt pseudo-labeling [9], [2], [32], [6], [45], which is another popular method of SSL that can be treated as a variant of consistent regularization. MixMatch [2] uses a series of data augmentations and applies consistency regularization on unlabeled data. FixMatch [32] sets a confidence threshold to filter the low quality pseudo-labels. Some SSL methods [28], [29], [32] believe that data augmentations are very important to SSL.

SSL for 2D and 3D Object Detection Recently, there has been lots of works [14], [50], [40], [33], [10], [15], [34], [51], [11], [27] in 2D Semi-Supervised Object Detection (SS-OD). Previous works have transferred a great deal of experience from SSL works to the SS-OD domain. STAC [33] uses Faster-RCNN [26] as its detector and trains the teacher model with the labeled data and generates pseudo-labels on unlabeled data as a static teacher. But with the accuracy of the student model, improving static pseudo-labels might lead to the opposite effect. Unbiased Teacher [14] solves the pseudo-labels bias problem caused by the class imbalance in real labels and the overfitting problem caused by the lack of labeled data. Unbiased Teacher v2 [15] aims at solving the ineffectiveness of the default regression supervision in semi-supervised, focusing on optimization by predicting the uncertainty of the boundary and achieving high performance under both anchor-based and anchor-free frameworks. Soft Teacher [40] proposes a soft teacher and box jitter mechanism, the former can directly assess all the box candidates from the student model, and the latter can select accurate pseudo boxes for the unlabeled regression. Dense Teacher [50] proposes a united form of pseudo-labels named DPL to fit the semi-supervised setting better. PseCo [10] proposes multi-scale feature alignment, which can be regarded as a kind of data augmentation. As for 3D Semi-Supervised Object Detection [48], [38], [20], [47], [43], [39], [12], SESS [48] is the pioneer in applying the SSL framework to point-based 3D object detection. It uses an EMA teacher and a student on top of VoteNet [21], asymmetric data augmentations, and three kinds of consistency losses between the predictions of the teacher and the student. 3DIoUMatch [38] proposes a multiple threshold filter strategy based on the SESS [48]. ATF-3D [47] proposes adaptive thresholds based on distance and confidence. DetMatch [20] jointly leverages the information of RGB images and point clouds with the Hungarian Matching algorithm [8] to get higher performance. Compared with the above methods, our DDS3D does not require additional image information.

III. METHOD

As shown in Fig. 2, we present the proposed framework of DDS3D, which contains three components: a) Teacher-Student network, b) dense pseudo-label generation, c) dynamic threshold selection. Before introducing the technical details of our DDS3D, we first provide the basic definitions for semi-supervised 3D object detection. In semi-supervised 3D object detection, the total dataset includes a small part of labeled data $\{x_i^l, y_i^l\}_{i=1}^{N_l}$ and a large amount of unlabeled

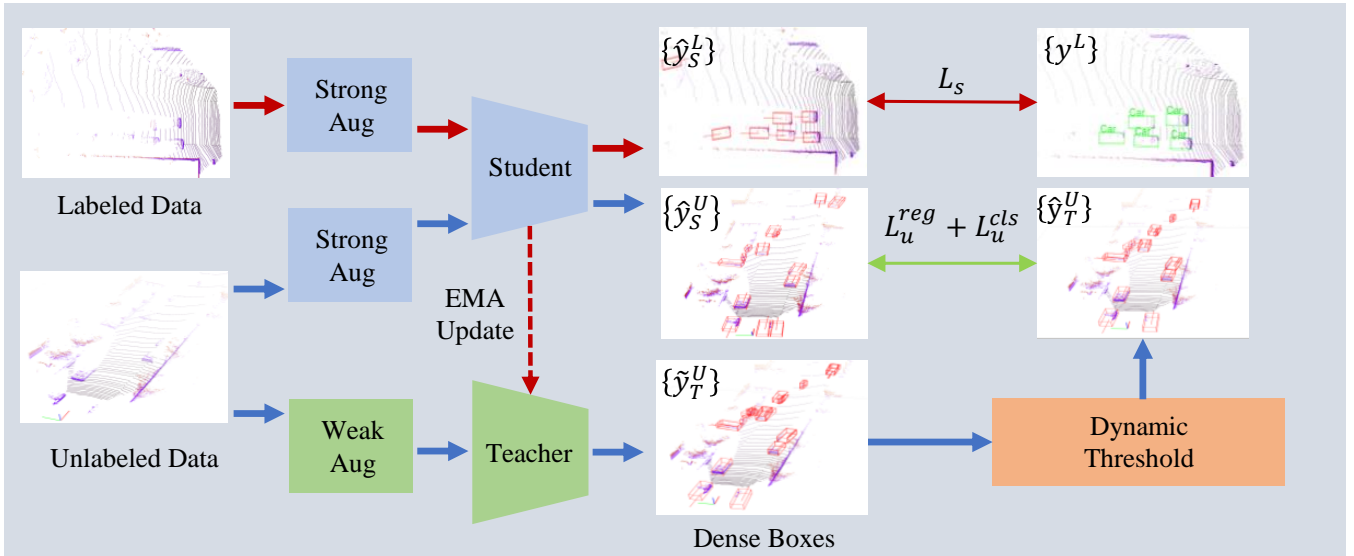


Fig. 2. **The pipeline of our semi-supervised framework.** For SSL, we utilize a teacher-student framework composed of a learnable student and an EMA teacher. For labeled data, the student network is supervised by GT labels directly. For unlabeled data, the student network is supervised by pseudo-labels from the EMA teacher. To get better results, we discard NMS and get dense predictions, and the gradient descent threshold is then applied to screen high-quality pseudo-labels.

data $\{x_i^u\}_{i=1}^{N_u}$, where N_l and N_u are the number of labeled and unlabeled data, respectively. x_i^l and y_i^l represent the input point cloud data and the corresponding ground truth annotations.

A. Framework of DDS3D

1) *Teacher-student Network:* Our DDS3D employs a teacher-student framework, where both the teacher network and the student network use the same 3D detector PV-RCNN [30] except for weight parameters and asymmetric data augmentation. More concretely, the teacher first feeds the unlabeled data with weak augmentation into the trained detector to produce the pseudo-labels, which are then utilized to supervise the student network. To ensure the effectiveness of semi-supervised learning, the pseudo-labels generated by the teacher network in the training stage are usually more accurate than the predictions of the student network. To this end, we adopt the EMA strategy during the training process.

$$\theta_T = \alpha \theta_T + (1 - \alpha) \theta_S \quad (1)$$

where α is the EMA momentum and θ_T and θ_S are the teacher and student model parameters respectively.

B. Dense Pseudo Label Generation

For obtaining pseudo labels, the previous methods [38], [48], [33] usually introduce NMS operation to remove redundant boxes and obtain high-quality pseudo labels. However, these approaches might be sub-optimal through employing NMS to deduplicate teacher predictions since some beneficial boxes may be removed in this process. The reason for this is the inconsistency of the classification scores and the quality of regressed boxes. Fig. 3 (a) and (b) illustrate the relationship among the classification score, IoU prediction

score and ground-truth 3D IoU in our teacher network (PV-RCNN). Although the IoU prediction is more reasonable than the classification score prediction, the prediction is still unsatisfactory compared with the ground truth. Thus, directly adopting pseudo-labels to supervise this IoU estimation branch will lead to inaccurate estimation and poor performance.

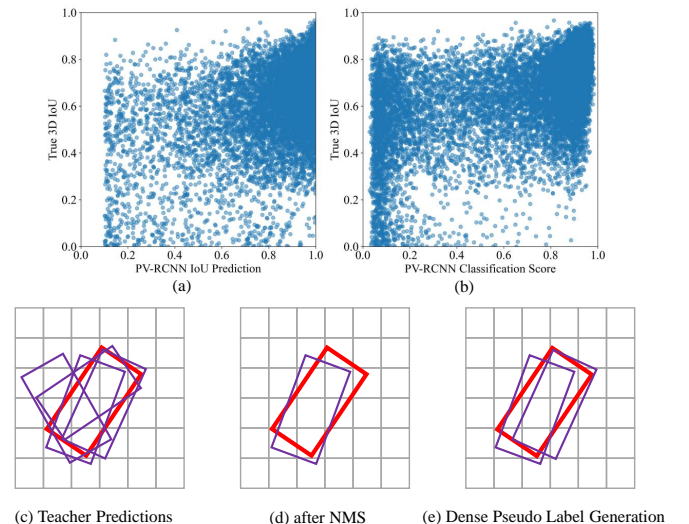


Fig. 3. Comparison of classification confidence and IoU estimation with true 3D IoU on KITTI validation set, PV-RCNN is trained with 1% labeled data; Pictorial illustration of NMS and Dense Pseudo Label Generation.

To alleviate this problem, we propose a simple and effective dense pseudo-label generation strategy. More concretely, we retain all proposals instead of filtering out many redundant boxes by NMS operation. As a result, a ground-truth object might be detected by multiple PV-RCNNs in this setting,

which naturally improves the recall of detection to provide more potential supervision information than these sparse pseudo-labels obtained from NMS operation. To illustrate this process better, we provide the visualization in Fig. 3, where (c) represents the proposals from the teacher, where (c) represents the proposals from the teacher. When NMS is used to process these proposals shown in Fig. 3 (d), this does not guarantee the generation of a high-quality box, which might lead to an unsatisfactory result. However, our dense pseudo label generation (see Fig. 3 (e)) can capture dense boxes to provide more potential information.

C. Dynamic Threshold Selection

The main gap in detection performance between these two networks in the teacher-student framework is from the different EMA weights and the data augmentation strength. Although the teacher network is usually more powerful than the student network, this does not guarantee that the teacher’s prediction is always more accurate than the student’s. A naive method is to use a fixed threshold to filter out low-quality pseudo-labels from the teacher network. As shown in Fig. 4, the threshold is set at a high value (e.g., 0.7 and 0.9), leading to more false negative examples. Conversely, when the threshold is set at a low value (e.g., 0.1 and 0.3), the performance of the model drop drastically due to a large number of false positive. To avoid this phenomenon, different from the fixed threshold methods [38], [32], we propose a dynamic threshold strategy. Specifically, we set a higher threshold to filter out most false positives to ensure the accuracy of the initial optimization direction. Then, as the number of iterations increases, we gradually reduce the threshold to retain more potential true positives due to the stronger detection performance. Especially at the end of the training, the model usually performs better on object localization. Therefore, a lower threshold is reasonable to cover more hard objects to further boost the performance on these challenging objects. Finally, the process of the dynamic threshold selection can be formulated as:

$$\sigma_{cls}(t) = \min \left(\sigma_{start} - \alpha \times \left\lfloor \frac{t}{steps} \right\rfloor, \sigma_{end} \right)$$

where $\sigma_{cls}(t)$ is the threshold for classification confidence at the number of iterations t , σ_{start} is the starting threshold, σ_{end} is the end threshold, $steps$ is step length and α is the attenuation coefficient default as 0.1.

D. Loss Function and Final Processing of Pseudo-Label

In the pre-training stage, we can use a small amount of labeled data $\{x_i^l, y_i^l\}_{i=1}^{N_l}$ to train the student network. The total loss in this stage L_l is composed of RPN losses and RCNN losses, as:

$$L_l = L_{rpn.cls}^l + L_{rpn.reg}^l + L_{rcnn.iou}^l + L_{rcnn.reg}^l \quad (4)$$

where $L_{rpn.cls}^l$ is classification loss, $L_{rcnn.iou}^l$ is IoU estimation loss, $L_{rpn.reg}^l$ and $L_{rcnn.reg}^l$ are box regression losses.

In the semi-supervised training stage, we keep the same proportion for the input labeled data and unlabeled data on each batch. For labeled data, we supervise the student with

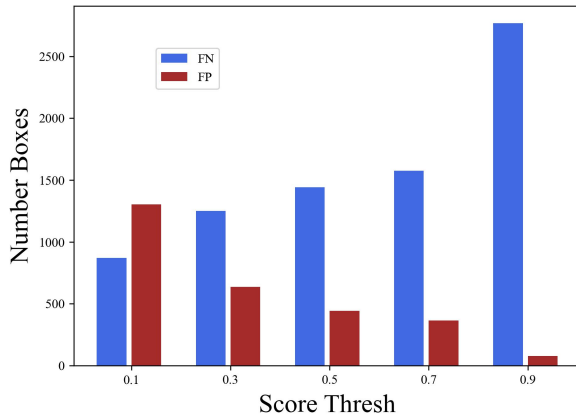


Fig. 4. The number of FP and FN under different classification confidence thresholds for the KITTI validation dataset.

GT (same with the pre-training stage). But for unlabeled data, given that the asymmetric data augmentation on unlabeled data for teacher and student, pseudo-labels need to go through additional geometry transformation \mathcal{T} to enable the alignment with outputs of the student network. \mathcal{T} is equal to the multiplication of the inverse weak augmentation and strong augmentation. Considering IoU is hard to optimize over the network, we remove the IoU estimation branch in the semi-supervised training stage. Thus, the total unsupervised loss L_u is composed of classification loss and box regression losses, which can be computed as follows.

$$L_u = L_{rpn.cls}^u + L_{rpn.reg}^u + L_{rcnn.reg}^u \quad (5)$$

Finally, the total loss L for semi-supervised framework is as follows.

$$L = L_l + \lambda L_u \quad (6)$$

Where λ is the balance weight of the unsupervised loss.

IV. EXPERIMENTS

A. Experimental Setup

Dataset and Evaluation Metrics. KITTI [5] dataset is a common dataset for autonomous driving, which contains 7481 training samples and 7518 testing samples. Following F-PointNet [22], the training samples are further divided into a *train* split (3712 samples) and a *val* split (3769 samples). For a fair comparison, We select the 1% and 2% labeled samples from *train* split following [38] to verify the effectiveness of our method. The mean Average Precision (mAP) with 40 recall positions is regarded as our evaluation metric. The IoU threshold for cars, pedestrians, and cyclists is set as 0.7, 0.5, and 0.5, respectively.

Implementation Details. We implement the basic detector PV-RCNN [30] based on the open-source framework OpenPCDet [37] codebase. In detail, the detection range is within [0, 70.4], [-40, 40], [-3, 1] meters along the X, Y, Z axes and the voxel size is (0.05, 0.05, 0.1) meters. The training process contains a pre-training stage and a training stage, and we train all models on 4 NVIDIA RTX 2080Ti GPUs.

TABLE I

THE PERFORMANCE FOR CAR, PEDESTRIAN AND CYCLIST ON THE KITTI *val* SET WITH DIFFERENT LEARNED RATIOS. **PEDE.** AND **CYC.** ARE SHORT FOR PEDESTRIAN AND CYCLIST. * DENOTES THE REPRODUCED RESULTS.

Method	1%			2%		
	Car	Ped.	Cyc.	Car	Ped.	Cyc.
PV-RCNN	73.5	28.7	28.4	76.6	40.8	45.5
PV-RCNN*	73.3	29.0	30.5	76.5	43.2	43.4
3DIoUMatch	76.0	31.7	36.4	78.7	48.2	56.2
3DIoUMatch*	76.0	30.7	36.8	78.6	45.3	53.0
DDS3D (Ours)	76.0	34.8	38.5	78.9	49.4	53.9

For the pre-training stage, we use the labeled data to train our model for 80 epochs with batch size of 8 (default 2 samples per GPU), and we train the data ten times per epoch so that the model converges better. The detector is optimized by AdamW [19] optimizer with a max learning rate of 0.01.

For the training stage, we run 100 epochs with batch size of 8 for 4 GPUs (each GPU loads 1 labeled sample and 1 unlabeled sample in each batch). Besides, we lengthen the number of traverses in each epoch to five times the origin following [38]. Similar to prior works [48], [38], we warm up the EMA momentum from 0.99 to 0.999. For our Dynamic Threshold Strategy, we set σ_{start} to 0.6, σ_{end} to 0.4 and *steps* to 1000. Further, for a fair comparison, we adopt the same data augmentations as 3DIoUMatch, including the GT Sampling for labeled data and basic geometric transformations for unlabeled data. The basic geometric involves random flip along the X axis, random global scaling with a scale factor sampled from $[0.95, 1.05]$, and global rotation around Z axis with a random angle sampled from $[-\frac{\pi}{4}, +\frac{\pi}{4}]$.

B. Results on KITTI

As shown in Table I, we provide a comparison with the superior semi-supervised 3D object detection method 3DIoUMatch under the settings of 1% and 2% labeled data on the KITTI [5] *val* split. For a fair comparison, we use the same detector PV-RCNN [30] as the labeled-data-only baseline. In Table I, our method outperforms the labeled-data-only baseline by 2.7%, 5.8% and 8.0% on cars, pedestrians and cyclists under 1% labeled data. Besides, our DDS3D achieves 3.1% and 2.1% mAP improvement over 3DIoUMatch [38] on pedestrians and cyclists, which illustrates the superiority of our DDS3D by considering the dense pseudo-label generation and the dynamic threshold strategies. Similar conclusions for 2% of the labeled data. For cars, our DDS3D achieves similar performance to 3DIoUMatch. The reason behind is that the detector on the category of the car has already achieved satisfactory results in the pre-training stage, which is difficult to improve by pseudo-labels in the semi-supervised framework.

C. Ablation Study

We present ablation studies with 1% labeled data to analyze the effectiveness of our proposed components in DDS3D

TABLE II

THE ABLATION OF THE IMPROVEMENT OF EACH COMPONENT ON THE KITTI *val* SET. SSL, FT, DT AND DPLG DENOTE SEMI-SUPERVISED LEARNING, FIXED THRESHOLD, DYNAMIC THRESHOLD AND DENSE PSEUDO-LABEL GENERATION. **PEDE.** AND **CYC.** ARE SHORT FOR PEDESTRIAN AND CYCLIST.

Exp ID	SSL	FT	DT	DPLG	Car	Ped.	Cyc.
a					73.3	29.0	30.5
b	✓				75.0	30.8	33.5
c	✓	✓			75.6	33.3	34.6
d	✓		✓		76.0	34.2	34.0
e	✓	✓		✓	76.0	34.4	36.0
f (ours)	✓		✓	✓	76.0	34.8	38.5

on KITTI [5] *val* split. Table II summarizes the ablation results on our dense pseudo-label generation mode (DPLG) and dynamic threshold module (DT). We adopt the labeled-data-only PV-RCNN as the baseline (Exp (a) of Table II). To validating the effectiveness of the dynamic threshold filter, we add a fixed threshold (FT) manner as a comparison. SSL stands for paradigm using semi-supervised learning.

Effect of dense pseudo label generation module. Compared with the naive pseudo-label baseline with a fixed threshold (Exp (c) of Table II), our dense pseudo-label generation (Exp (e) of Table II) achieves 0.4%, 1.1% and 1.4% mAP on car, pedestrian and cyclist, respectively. The main reason is that some boxes with high IoU with GT but low scores are filtered out by NMS as redundant boxes. Our dense pseudo-label generation mode can effectively deal with this case.

Effect of dynamic threshold. For a fair comparison, we extensively search for the fixed confidence threshold, as shown in Table III. It is worth noting that different optimal thresholds might be required for different object classes. To reduce the number of hyperparameters, we use the same threshold to filter all categories. As shown in Table III, setting the fixed threshold to 0.4 is a reliable choice. Thus, we choose the value of 0.4 as the fixed threshold Table II. Compared with our baseline with the fixed threshold Table II (exp (c)), our dynamic threshold strategy shown in Table II (exp (d)) achieves 0.4% mAP improvement on cars and 0.9% mAP improvement on pedestrians. Moreover, our dynamic threshold strategy with dense pseudo label generation brings a significant improvement to the fixed threshold, which achieves 0.4% mAP improvement on pedestrians and 2.5% mAP improvement on cyclists. The naive pseudo-label baseline proves that directly using teachers' proposals as pseudo-labels to supervise the student model gets low-performance improvement. On the other hand, it is proven that supervision with high quality and sufficient pseudo-labels is necessary. Therefore, it demonstrates the effectiveness of our dynamic threshold and more details will be discussed in later sections.

Effect of different threshold strategies Table IV shows the performance of our dynamic threshold strategy under different settings, and all experiments are trained for 60

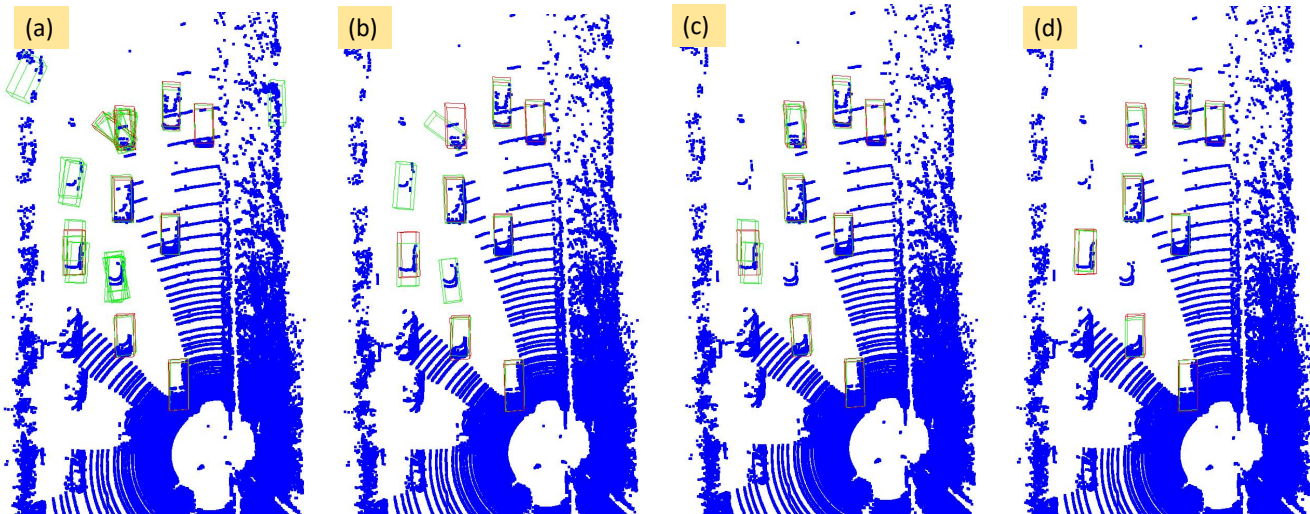


Fig. 5. The Visualization of detection results on the KITTI dataset. (a), (b), (c) and (d) denote teacher’s proposals, sparse pseudo-labels, dense pseudo-labels and prediction results. The prediction and GT are in green and red, respectively.

TABLE III

THE ABLATION OF THE FIXED AND DYNAMIC THRESHOLD.

Threshold	Car	Pedestrian	Cyclist	mAP
0.3	75.0	31.8	32.8	46.5
0.4	75.6	33.3	34.6	47.8
0.5	76.2	29.4	34.9	46.8
0.6	74.0	24.7	30.0	42.9
DT (Ours)	76.0	34.8	38.5	49.8

TABLE IV

THE ABLATION OF THE RANGE OF THE DYNAMIC THRESHOLD (DT).

Range of DT	Car	Pedestrian	Cyclist	mAP
0.4→0.6	75.7	31.9	34.5	47.4
0.6→0.4	75.8	34.5	36.8	49.0
0.7→0.3	75.8	36.2	35.4	49.1
0.8→0.3	76.2	35.0	35.7	49.0

epochs with *steps* as 500. We design some different start and end of the dynamic threshold strategy and different threshold trends: high-to-low (our dynamic strategy) and low-to-high. According to the result, our dynamic threshold strategy always works well no matter how we choose the start and end. Moreover, we proposed high-to-low dynamic threshold strategy brings effective improvement, but the low-to-high strategy drops the performance, which demonstrates the effectiveness of our proposed dynamic threshold strategy and our hypothesis about the SSL that in the early training stage, the teacher needs a higher threshold to filter out wrong predictions that are going to be pseudo-labels, which ensures the accuracy of the initial optimization direction, and in the latter training stage, the teacher needs lower threshold to keep more predictions, which covers more hard objects so as to further boost the performance on these challenging objects.

D. Qualitative Results and Analysis

Fig. 5 shows the visualizations of the predictions by PV-RCNN [30], 3DIoUMatch [38], and DDS3D with 2% labeled data on the KITTI [5] dataset the bird’s-eye view. As shown in Fig. 5, (a) generates the pseudo labels from the teacher network PV-RCNN before NMS operation. (b) shows the sparse predictions from 3DIoUMatch through filtering out (a) in NMS operation, whose high-quality objects are obtained by the score ranking in NMS. Thus, some high-quality but low-score boxes may be eliminated due to the inconsistency between the confidence scores and the quality of the regressed boxes. (c) represents our dense pseudo-label generation strategy, which keeps more high-quality boxes compared to sparse pseudo-labels. (d) shows the final pseudo labels produced by our DDS3D, where all objects can be accurately localized. This effectively illustrates our dense pseudo labels are more reliable than traditional sparse pseudo labels.

V. CONCLUSION

In this paper, we have presented a novel semi-supervised 3D object detection framework named DDS3D, which involves a dense pseudo-label generation mode and a dynamic threshold strategy. The dense pseudo label generation can retain more beneficial pseudo labels compared with the manner of filtering out a large number of redundant pseudo labels through NMS operation. Besides, the proposed dynamic threshold strategy can effectively adjust a proper threshold to cover more reliable pseudo labels, which is essential for our teacher-student semi-supervised framework. Finally, DDS3D outperforms the state-of-the-art method on 1% labeled data under the same settings, and the experiment results on the KITTI dataset validate the effectiveness of these two components in our DDS3D. In the future, we hope that our DDS3D can be extended to more 2D/3D semi-supervised 3D object detection frameworks.

REFERENCES

- [1] David Berthelot, Nicholas Carlini, Ekin D Cubuk, Alex Kurakin, Kihyuk Sohn, Han Zhang, and Colin Raffel. Remixmatch: Semi-supervised learning with distribution alignment and augmentation anchoring. In *Proc. of International Conference on Learning Representations*, 2020.
- [2] David Berthelot, Nicholas Carlini, Ian Goodfellow, Nicolas Papernot, Avital Oliver, and Colin A Raffel. Mixmatch: A holistic approach to semi-supervised learning. *Advances in neural information processing systems*, 32, 2019.
- [3] Jiajun Deng, Shaoshuai Shi, Peiwei Li, Wengang Zhou, Yanyong Zhang, and Houqiang Li. Voxel r-cnn: Towards high performance voxel-based 3d object detection. In *Proc. of the AAAI Conf. on Artificial Intelligence*, volume 35, pages 1201–1209, 2021.
- [4] Shuang Deng, Qiulei Dong, Bo Liu, and Zhanyi Hu. Superpoint-guided semi-supervised semantic segmentation of 3d point clouds. In *2022 International Conference on Robotics and Automation (ICRA)*, pages 9214–9220. IEEE, 2022.
- [5] Andreas Geiger, Philip Lenz, and Raquel Urtasun. Are we ready for autonomous driving? the kitti vision benchmark suite. In *Proc. of IEEE Intl. Conf. on Computer Vision and Pattern Recognition*, pages 3354–3361. IEEE, 2012.
- [6] Benjamin Graham, Martin Engelcke, and Laurens Van Der Maaten. 3d semantic segmentation with submanifold sparse convolutional networks. In *Proceedings of the IEEE conference on computer vision and pattern recognition*, pages 9224–9232, 2018.
- [7] Tengpeng Huang, Zhe Liu, Xiwu Chen, and Xiang Bai. Epnet: Enhancing point features with image semantics for 3d object detection. In *Proc. of European Conference on Computer Vision*, pages 35–52. Springer, 2020.
- [8] Harold W Kuhn. The hungarian method for the assignment problem. *Naval research logistics quarterly*, 2(1-2):83–97, 1955.
- [9] Dong-Hyun Lee et al. Pseudo-label: The simple and efficient semi-supervised learning method for deep neural networks. In *Workshop on challenges in representation learning, ICML*, volume 3, page 896, 2013.
- [10] Gang Li, Xiang Li, Yujie Wang, Shanshan Zhang, Yichao Wu, and Ding Liang. Pseco: Pseudo labeling and consistency training for semi-supervised object detection. In *Proc. of European Conference on Computer Vision*, 2022.
- [11] Hengduo Li, Zuxuan Wu, Abhinav Shrivastava, and Larry S Davis. Rethinking pseudo labels for semi-supervised object detection. In *Proc. of the AAAI Conf. on Artificial Intelligence*, volume 36, pages 1314–1322, 2022.
- [12] Peixuan Li and Huaici Zhao. Monocular 3d detection with geometric constraint embedding and semi-supervised training. *IEEE Robotics and Automation Letters*, 6(3):5565–5572, 2021.
- [13] Chuandong Liu, Chenqiang Gao, Fangcen Liu, Jiang Liu, Deyu Meng, and Xinbo Gao. Ss3d: Sparsely-supervised 3d object detection from point cloud. In *Proc. of IEEE Intl. Conf. on Computer Vision and Pattern Recognition*, pages 8428–8437, 2022.
- [14] Yen-Cheng Liu, Chih-Yao Ma, Zijian He, Chia-Wen Kuo, Kan Chen, Peizhao Zhang, Bichen Wu, Zsolt Kira, and Peter Vajda. Unbiased teacher for semi-supervised object detection. In *Proc. of International Conference on Learning Representations*, 2020.
- [15] Yen-Cheng Liu, Chih-Yao Ma, and Zsolt Kira. Unbiased teacher v2: Semi-supervised object detection for anchor-free and anchor-based detectors. In *Proc. of IEEE Intl. Conf. on Computer Vision and Pattern Recognition*, pages 9819–9828, 2022.
- [16] Zhe Liu, Tengpeng Huang, Bingling Li, Xiwu Chen, Xi Wang, and Xiang Bai. Epnet++: Cascade bi-directional fusion for multi-modal 3d object detection. *IEEE Transactions on Pattern Analysis and Machine Intelligence*, 2022.
- [17] Zhe Liu, Xiaoqing Ye, Xiao Tan, Errui Ding, and Xiang Bai. Stereodistill: Pick the cream from lidar for distilling stereo-based 3d object detection. In *Proc. of the AAAI Conf. on Artificial Intelligence*, 2023.
- [18] Zhe Liu, Xin Zhao, Tengpeng Huang, Ruolan Hu, Yu Zhou, and Xiang Bai. Tanet: Robust 3d object detection from point clouds with triple attention. In *Proc. of the AAAI Conf. on Artificial Intelligence*, volume 34, pages 11677–11684, 2020.
- [19] Ilya Loshchilov and Frank Hutter. Decoupled weight decay regularization. *arXiv preprint arXiv:1711.05101*, 2017.
- [20] Jinhung Park, Chenfeng Xu, Yiyang Zhou, Masayoshi Tomizuka, and Wei Zhan. Detmatch: Two teachers are better than one for joint 2d and 3d semi-supervised object detection. In *Proc. of European Conference on Computer Vision*, 2022.
- [21] Charles R Qi, Or Litany, Kaiming He, and Leonidas J Guibas. Deep hough voting for 3d object detection in point clouds. In *Proc. of IEEE Intl. Conf. on Computer Vision*, pages 9277–9286, 2019.
- [22] Charles R Qi, Wei Liu, Chenxia Wu, Hao Su, and Leonidas J Guibas. Frustum pointnets for 3d object detection from rgb-d data. In *Proceedings of the IEEE conference on computer vision and pattern recognition*, pages 918–927, 2018.
- [23] Charles Ruizhongtai Qi, Li Yi, Hao Su, and Leonidas J Guibas. Pointnet++: Deep hierarchical feature learning on point sets in a metric space. *Advances in neural information processing systems*, 30, 2017.
- [24] Charles R Qi, Yin Zhou, Mahyar Najibi, Pei Sun, Khoa Vo, Boyang Deng, and Dragomir Anguelov. Offboard 3d object detection from point cloud sequences. In *Proc. of IEEE Intl. Conf. on Computer Vision and Pattern Recognition*, pages 6134–6144, 2021.
- [25] Antti Rasmus, Mathias Berglund, Mikko Honkala, Harri Valpola, and Tapani Raiko. Semi-supervised learning with ladder networks. *Advances in neural information processing systems*, 28, 2015.
- [26] Shaoqing Ren, Kaiming He, Ross Girshick, and Jian Sun. Faster r-cnn: Towards real-time object detection with region proposal networks. *Advances in neural information processing systems*, 28, 2015.
- [27] Mamshad Nayeem Rizve, Kevin Duarte, Yogesh S Rawat, and Mubarak Shah. In defense of pseudo-labeling: An uncertainty-aware pseudo-label selection framework for semi-supervised learning. In *Proc. of International Conference on Learning Representations*, 2020.
- [28] Mehdi Sajjadi, Mehran Javanmardi, and Tolga Tasdizen. Regularization with stochastic transformations and perturbations for deep semi-supervised learning. *Advances in neural information processing systems*, 29, 2016.
- [29] Laine Samuli and Aila Timo. Temporal ensembling for semi-supervised learning. In *Proc. of International Conference on Learning Representations*, volume 4, page 6, 2017.
- [30] Shaoshuai Shi, Chaoxu Guo, Li Jiang, Zhe Wang, Jianping Shi, Xiaogang Wang, and Hongsheng Li Pv-rnn. Point-voxel feature set abstraction for 3d object detection. 2020 ieee. In *Proc. of IEEE Intl. Conf. on Computer Vision and Pattern Recognition*, pages 10526–10535, 2020.
- [31] Shaoshuai Shi, Xiaogang Wang, and Hongsheng Li. Pointcnn: 3d object proposal generation and detection from point cloud. In *Proc. of IEEE Intl. Conf. on Computer Vision and Pattern Recognition*, pages 770–779, 2019.
- [32] Kihyuk Sohn, David Berthelot, Nicholas Carlini, Zizhao Zhang, Han Zhang, Colin A Raffel, Ekin Dogus Cubuk, Alexey Kurakin, and Chun-Liang Li. Fixmatch: Simplifying semi-supervised learning with consistency and confidence. *Advances in neural information processing systems*, 33:596–608, 2020.
- [33] Kihyuk Sohn, Zizhao Zhang, Chun-Liang Li, Han Zhang, Chen-Yu Lee, and Tomas Pfister. A simple semi-supervised learning framework for object detection. *arXiv preprint arXiv:2005.04757*, 2020.
- [34] Yihe Tang, Weifeng Chen, Yijun Luo, and Yuting Zhang. Humble teachers teach better students for semi-supervised object detection. In *Proceedings of the IEEE/CVF Conference on Computer Vision and Pattern Recognition*, pages 3132–3141, 2021.
- [35] Antti Tarvainen and Harri Valpola. Mean teachers are better role models: Weight-averaged consistency targets improve semi-supervised deep learning results. *Advances in neural information processing systems*, 30, 2017.
- [36] A Tarvainen and H Valpola. Weight-averaged consistency targets improve semi-supervised deep learning results. *corr abs/1703.01780*. *arXiv preprint arXiv:1703.01780*, 1(5), 2017.
- [37] OpenPCDet Development Team. Openpcdet: An open-source toolbox for 3d object detection from point clouds. <https://github.com/open-mmlab/OpenPCDet>, 2020.
- [38] He Wang, Yezhen Cong, Or Litany, Yue Gao, and Leonidas J Guibas. 3dioumatch: Leveraging iou prediction for semi-supervised 3d object detection. In *Proc. of IEEE Intl. Conf. on Computer Vision and Pattern Recognition*, pages 14615–14624, 2021.
- [39] Yi Wei, Shang Su, Jiwen Lu, and Jie Zhou. Fgr: Frustum-aware geometric reasoning for weakly supervised 3d vehicle detection. In *2021 IEEE International Conference on Robotics and Automation (ICRA)*, pages 4348–4354. IEEE, 2021.
- [40] Mengde Xu, Zheng Zhang, Han Hu, Jianfeng Wang, Lijuan Wang, Fangyun Wei, Xiang Bai, and Zicheng Liu. End-to-end semi-supervised object detection with soft teacher. In *Proc. of IEEE Intl. Conf. on Computer Vision*, pages 3060–3069, 2021.
- [41] Yan Yan, Yuxing Mao, and Bo Li. Second: Sparsely embedded convolutional detection. *Sensors*, 18(10):3337, 2018.
- [42] Zetong Yang, Yanan Sun, Shu Liu, and Jiaya Jia. 3dssd: Point-based 3d single stage object detector. In *Proc. of IEEE Intl. Conf. on Computer Vision and Pattern Recognition*, pages 11040–11048, 2020.

- [43] Mao Ye, Chenxi Liu, Maoqing Yao, Weiyue Wang, Zhaoqi Leng, Charles R. Qi, and Dragomir Anguelov. Multi-class 3d object detection with single-class supervision. In *2022 International Conference on Robotics and Automation (ICRA)*, pages 5123–5130, 2022.
- [44] Tianwei Yin, Xingyi Zhou, and Philipp Krahenbuhl. Center-based 3d object detection and tracking. In *Proc. of IEEE Intl. Conf. on Computer Vision and Pattern Recognition*, pages 11784–11793, 2021.
- [45] Bowen Zhang, Yidong Wang, Wenxin Hou, Hao Wu, Jindong Wang, Manabu Okumura, and Takahiro Shinozaki. Flexmatch: Boosting semi-supervised learning with curriculum pseudo labeling. *Advances in Neural Information Processing Systems*, 34:18408–18419, 2021.
- [46] Yifan Zhang, Qingyong Hu, Guoquan Xu, Yanxin Ma, Jianwei Wan, and Yulan Guo. Not all points are equal: Learning highly efficient point-based detectors for 3d lidar point clouds. In *Proc. of IEEE Intl. Conf. on Computer Vision and Pattern Recognition*, pages 18953–18962, 2022.
- [47] Zehan Zhang, Yang Ji, Wei Cui, Yulong Wang, Hao Li, Xian Zhao, Duo Li, Sanli Tang, Ming Yang, Wenming Tan, et al. Atf-3d: Semi-supervised 3d object detection with adaptive thresholds filtering based on confidence and distance. *IEEE Robotics and Automation Letters*, 7(4):10573–10580, 2022.
- [48] Na Zhao, Tat-Seng Chua, and Gim Hee Lee. Sess: Self-ensembling semi-supervised 3d object detection. In *Proc. of IEEE Intl. Conf. on Computer Vision and Pattern Recognition*, pages 11079–11087, 2020.
- [49] Wu Zheng, Weiliang Tang, Li Jiang, and Chi-Wing Fu. Se-ssd: Self-ensembling single-stage object detector from point cloud. In *Proc. of IEEE Intl. Conf. on Computer Vision and Pattern Recognition*, pages 14494–14503, 2021.
- [50] Hongyu Zhou, Zheng Ge, Songtao Liu, Weixin Mao, Zeming Li, Haiyan Yu, and Jian Sun. Dense teacher: Dense pseudo-labels for semi-supervised object detection. In *Proc. of European Conference on Computer Vision*, 2022.
- [51] Qiang Zhou, Chaohui Yu, Zhibin Wang, Qi Qian, and Hao Li. Instant-teaching: An end-to-end semi-supervised object detection framework. In *Proc. of IEEE Intl. Conf. on Computer Vision and Pattern Recognition*, pages 4081–4090, 2021.
- [52] Yin Zhou and Oncel Tuzel. Voxnet: End-to-end learning for point cloud based 3d object detection. In *Proc. of IEEE Intl. Conf. on Computer Vision and Pattern Recognition*, pages 4490–4499, 2018.